Structural Engineering and Mechanics, Vol. 6, No. 7 (1998) 817-826
DOI: http://dx.doi.org/10.12989/sem.1998.6.7.817

Finite element application of an incremental endochronic model to flexible pavement materials

Tienfuan Kerh† and C.Y. Huang‡

Department of Civil Engineering, National Pingtung University of Science and Technology, Pingtung, Taiwan 91207, R.O.C.

Abstract. A finite element model based on the incremental endochronic theory for flexible pavement materials was developed in this study. Three grid systems with eight-node cubic isoparametric elements, and different loading steps were used to perform the calculations for a specimen of circular cylinder. The uniaxial stress experimental results on an asphalt mixture at 60°C in SHRP conducted by University of California at Berkeley were used to check the ability of the derived numerical model. Then, the numerical results showed isotropic response and deviatoric response on the specimen in a three dimensional manner, which provided a better understanding for a deformed flexible material under the specified loading conditions.

Key words: finite element analysis; incremental endochronic theory; flexible pavement material; isotropic response; deviatoric response

1. Introduction

Pavement materials, such as asphalt concretes usually exist in the top layer of a road profile and play a key role for transmission of loading in the road foundation. The mechanical behavior of the pavement material may significantly influence the quality and the safety of a road system, and thus becomes a crucial issue in the field of road engineering. Early studies of road design in material behaviors were limited to experiments, which required many tests in the laboratory to obtain a series of useful data. Recently, theoretical and numerical analyses have become popular, such as hypoelastic analysis (e.g., Liue 1993, 1994) and visco-elastic analysis (e.g., Henrinksen 1984, Row *et al.* 1995) for the materials. Whereas, the results based on the elastic theory were unable to describe plastic behavior which exhibits permanent deformation. Thus, plastic theory in a modified form was developed and frequently employed in this field.

Classical plastic models consist of a yield criterion, yield surface change and associated or non-associated flow rules. The analysis must set up a yield surface, the stress within the surface can be considered as elastic, but when it reaches the surface, plastic behavior is in force and the strain should be obtained through the flow rules. However, the yield surface will change due to plastic deformation, and that is a serious problem for materials which exhibit plastic behaviors at the beginning of applied loading. Hence, the endochronic theory

† Professor
‡Graduate student

and its modification were developed for solving this problem and computational cost saving (Valanis 1971, 1980, 1984). The results were also applied successfully in several metal and porous materials under different loading conditions (Wu and Wang 1983, Valanis and Fan 1984, Watanabe and Atluri 1986, Sugiura *et al.* 1987, Wu and Aboutorabi 1988, Wu *et al.* 1990, Wu and Komarakulnanakorn 1992, Wu and Lu 1995). Detailed deviations of the endochronic theory and its extended form can be found in the above works.

Finite element analysis based on the endochronic plasticity is described in the recent report (e.g., Lee 1995), but the result focussed on steel material. The application of finite element method to flexible pavement material is rarely seen up to the present time. Therefore, the main purpose of this study is to develop a finite element model based upon the endochronic theory to describe the mechanical behaviors of pavement material. Basically, from the Gibbs free energy model, the isotropic response, the deviatoric response, the definitions of deviatoric stress and deviatoric strain are integrated to derive a new stress-strain relationship. The principle of virtual work is further employed to formulate the stress-strain equations. The governing equation in form of a finite element procedure is finally developed and can then be programmed and analyzed numerically for the mechanical responses of pavement materials. In performing the finite element analysis for this problem, it requires some of constants for the pavement material, so that the uniaxial stress experimental results on an asphalt mixture at 60°C described in a quarterly report (SHRP 1991) of University of California at Berkeley are used for the sake of comparisons. Next, a three dimensional circular cylinder of the pavement material is taken to study the isotropic and deviatoric effects under a specified loading. The variations of the whole specimen can be easily seen from the numerical profiles. These are better than the average results calculated directly from the theory itself. The developed finite element may also be applied to solve other problems in this field.

2. Derivation of finite element models

A complete stress-strain equation can be divided into an isotropic part and a deviatoric part. The isotropic and deviatoric parts can be combined together to obtain a complete stress-strain equation, which permits the application of a finite element methodology. The endochronic theory is based on Gibbs free energy model (see Wu and Aboutorabi 1988, Wu *et al.* 1990). From the definitions of incremental deviatoric strain (de_{ij}) and incremental deviatoric stress (dS_{ij}), the equations can be written as follows:

$$de_{ij} = d\varepsilon_{ij} - \frac{1}{3} d\varepsilon_{kk}\, \delta_{ij} \tag{1}$$

$$dS_{ij} = d\sigma_{ij} - \frac{1}{3} d\sigma_{kk}\, \delta_{ij} \tag{2}$$

where $d\sigma_{ij}$ is the increment of isotropic stress, $d\varepsilon_{ij}$ is the increment of isotropic strain, and δ_{ij} is the Kronecker's delta. For the incremental isotropic response and the incremental deviatoric response, the equations are:

$$d\varepsilon_{kk} = 3A_0 d\sigma_{kk} + 3B_0 d\gamma_{kk} \tag{3}$$

$$de_{ij} = A_1 dS_{ij} + C_1 dp_{ij} \tag{4}$$

where A_0, B_0, A_1 and C_1 are constants, γ_{kk} is the internal variable for isotropic deformation, p_{ij} is

the internal variable for deviatoric deformation, and the subscript *kk* (*k*=1 to 3) is the tensor index.

From the above equations, the following equation can be derived;

$$\begin{aligned} d\varepsilon_{ij} - \frac{1}{3} d\varepsilon_{kk}\delta_{ij} &= A_1 (d\sigma_{ij} - \frac{1}{3} d\sigma_{kk}\delta_{ij}) + C_1 dp_{ij} \\ &= A_1 \left[d\sigma_{ij} - \frac{1}{3}\cdot\frac{1}{3A_0}(d\varepsilon_{kk} - 3B_0 d\gamma_{kk})\delta_{ij} \right] + C_1 dp_{ij} \\ &= A_1 d\sigma_{ij} - \frac{A_1}{9A_0}(d\varepsilon_{kk} - 3B_0 d\gamma_{kk})\delta_{ij} + C_1 dp_{ij} \end{aligned} \tag{5}$$

or

$$A_1 d\sigma_{ij} = d\varepsilon_{ij} - \frac{1}{3} d\varepsilon_{kk}\delta_{ij} + \frac{A_1}{9A_0} d\varepsilon_{kk}\delta_{ij} - \frac{A_1 B_0}{3A_0} d\gamma_{kk}\delta_{ij} - C_1 dp_{ij} \tag{6}$$

Let $A_2 = \frac{1}{A_1}$ and $A_3 = \frac{1}{A_1}(\frac{1}{3} - \frac{A_1}{9A_0})$, it can be shown that

$$d\sigma_{ij} = A_2 d\varepsilon_{ij} - A_3 d\varepsilon_{kk}\delta_{ij} - \frac{B_0}{3A_0} d\gamma_{kk}\delta_{ij} - \frac{C_1}{A_1} dp_{ij} \tag{7}$$

In order to implement a finite element method, the above equation can be written in matrix form as:

$$\{d\sigma\} = [D]\{d\varepsilon\} + \{dHP\} \tag{8}$$

and the complete equation is:

$$\begin{bmatrix} d\sigma_{11} \\ d\sigma_{22} \\ d\sigma_{33} \\ d\sigma_{12} \\ d\sigma_{13} \\ d\sigma_{23} \end{bmatrix} = \begin{bmatrix} A_2 - A_3 & -A_3 & -A_3 & 0 & 0 & 0 \\ -A_3 & A_2 - A_3 & -A_3 & 0 & 0 & 0 \\ -A_3 & -A_3 & A_2 - A_3 & 0 & 0 & 0 \\ 0 & 0 & 0 & A_2 & 0 & 0 \\ 0 & 0 & 0 & 0 & A_2 & 0 \\ 0 & 0 & 0 & 0 & 0 & A_2 \end{bmatrix} \begin{bmatrix} d\varepsilon_{11} \\ d\varepsilon_{22} \\ d\varepsilon_{33} \\ d\varepsilon_{12} \\ d\varepsilon_{13} \\ d\varepsilon_{23} \end{bmatrix} + \begin{bmatrix} -\frac{B_0}{3A_0} d\gamma_{kk} - \frac{C_1}{A_1} dp_{11} \\ -\frac{B_0}{3A_0} d\gamma_{kk} - \frac{C_1}{A_1} dp_{22} \\ -\frac{B_0}{3A_0} d\gamma_{kk} - \frac{C_1}{A_1} dp_{33} \\ -\frac{C_1}{A_1} dp_{12} \\ -\frac{C_1}{A_1} dp_{13} \\ -\frac{C_1}{A_1} dp_{23} \end{bmatrix} \tag{9}$$

Now, from the principle of virtual; work and the stress-strain with strain-displacement relations, the governing equation can be written as:

$$\int_V \sigma_{ij}\ \delta\varepsilon_{ij}\ dV = T_i\ \delta u_i \tag{10}$$

whrer δu_i and $\delta\varepsilon_{ij}$ are the increment of virtual displacement and the increment of virtual strain, respetively. T_i is the external force on the element, and V is the volume of the element. By neglecting the effect of material weight as it is very small when compared to the external force, the above equation in the matrix form is

$$\int_V \{d\sigma\}_E^T \{\delta\varepsilon\}_E\ dV = \{dT\}_E^T \{\delta u\} \tag{11}$$

Furthermore, the relations of stress-strain and strain-displacement in an element basis (subscript E) have the following equations:

$$\{d\sigma\}_E = [D]\{d\varepsilon\}_E + \{dHP\}_E \tag{12}$$

$$\{d\varepsilon\}_E = [B]\{du\}_E \tag{13}$$

where $[B]$ is the strain-displacement matrix and can be computed from shape functions of the chosen element. From Eqs. (15) to (17), it can be obtained that

$$[\{du\}_E^T \int_V [B]^T\ [D][B]\ dV - \{dT\}_E^T + \int_V \{dHP\}^T\ [B]\ dV]\ \{\delta u\}_E = 0 \tag{14}$$

The above equation is true for any virtual displacement, thus

$$\int_V [B]^T\ [D][B]\ dV\ \{du\}_E = \{dT\}_E - \int_V [B]^T\ \{dHP\}\ dV \tag{15}$$

or

$$[K]_E\ \{du\}_E = \{dT\}_E - \{dPF\}_E \tag{16}$$

where the element stiffness matrix and the plastic pseudo-force vector are:

$$[K]_E = \int_V [B]^T\ [D]\ [B]\ dV \tag{17}$$

$$[dPF]_E = \int_V [B]^T\ \{dHP\}\ dV \tag{18}$$

By assembling the element matrix, the global equation (subscript E is dropped) can be written as:

$$[K]\ \{du\} = \{dT\} - \{dPF\} \tag{19}$$

where $\{du\}$ is the unknown vector of nodal displacements. Once the element type is chosen, the matrices can be computed numerically by using Gauss quadrature. For example, eight Gauss points are required to integrate a brick element (8-node) for the $[K]$ matrix exactly. From Eq. (23), the resulting system of equations can be solved by using direct Gaussian elimination, and the other variables can then be computed accordingly.

3. Discussion of numerical results

In order to perform the numerical analysis, a uniaxial stresss test on an asphalt mixture at 60°C carried out by SHRP (Strategic Highway Research Program, an asphalt research project conducted by University of California at Berkeley) is used for the sake of comparison. For the chosen material, the constants are obtained using curve fitting to satisfy the stress-strain relations, and the most important coefficients such as the Young's modulus E=10,000kPa and Poisson ratio ν=0.19 are used in this study. The other coefficients for the endochronic theory can be obtained similarly. Note that the values of elastic bulk modulus K=180000 kPa and elastic shear modulus G=140672 kPa for the present study lie in a reasonable range, which conforms to the relationship $G \leq (3/2)K$, where $K/G=2(1+\nu)/3(1-2\nu)$ and $0 \leq \nu < 0.5$.

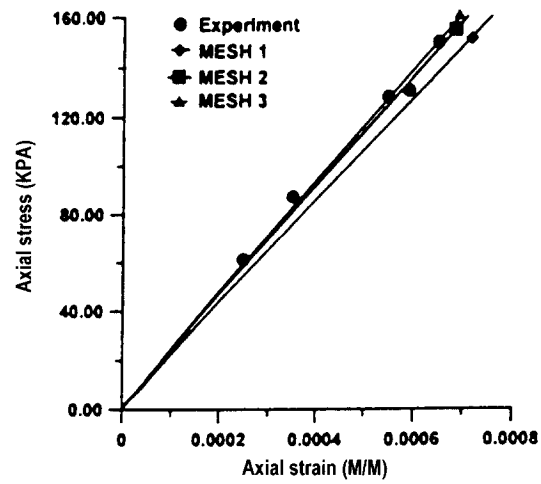

Fig. 1 Finite element results compared to experimental data (SHRP, uniaxial test) for different grid systems

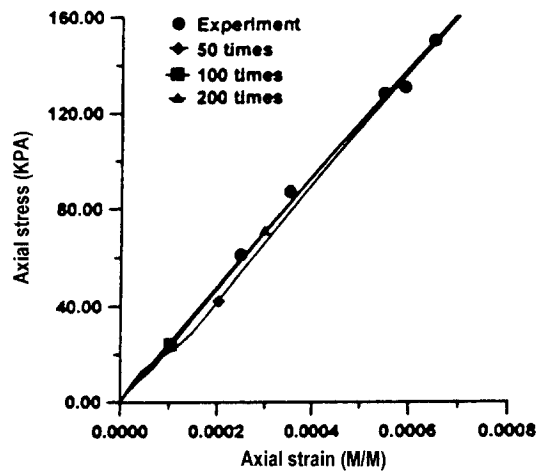

Fig. 2 Finite element results compared to experimental data (SHRP, uniaxial test) for different loading steps

Consider a circular cylinder, 4 inches in diameter. Because of symmetry, only one half of the cylinder is taken as the specimen for analysis. Three grid systems are considered with eight-node cubic isoparametric elements used to model the specimen. The meshes are: $2\times 2\times 3$ elements for mesh 1, $3\times 3\times 3$ elements for mesh 2, and $4\times 4\times 3$ elements for mesh 3, which result in 36 nodes, 64 nodes and 100 nodes for the three grid system, respectively. In each grid system, three elements is used to devide the specimen in the z-direction, so that four layers (including top layer and bottom layer) can be used for analysis. In addition, when considering compression of the cylinder, the boundary conditions are constrained for the loading contact surface (top layer, x-y plane), but due to symmetry and only one half of the cylinder is considered for the calculation, the boundary conditions in the z-direction are constrained and set to zero values for the bottom surface. In Fig. 1, the numerical results are compared with the experimemtal data of the uniaxial test for the three meshes. Good agreement is found for the three meshes, particularly for the finest mesh system. Since convergence for the elements is considered to be sufficient from the comparison, mesh 3 was used for other calculations.

Shown in Fig. 2 is the stress-strain curve under different loading steps. For instance, if the whole axial stress is P, then the increment of stress in each step is $P/200$. In each step, the value of strain can be obtained through numerical calculation, and the curve is

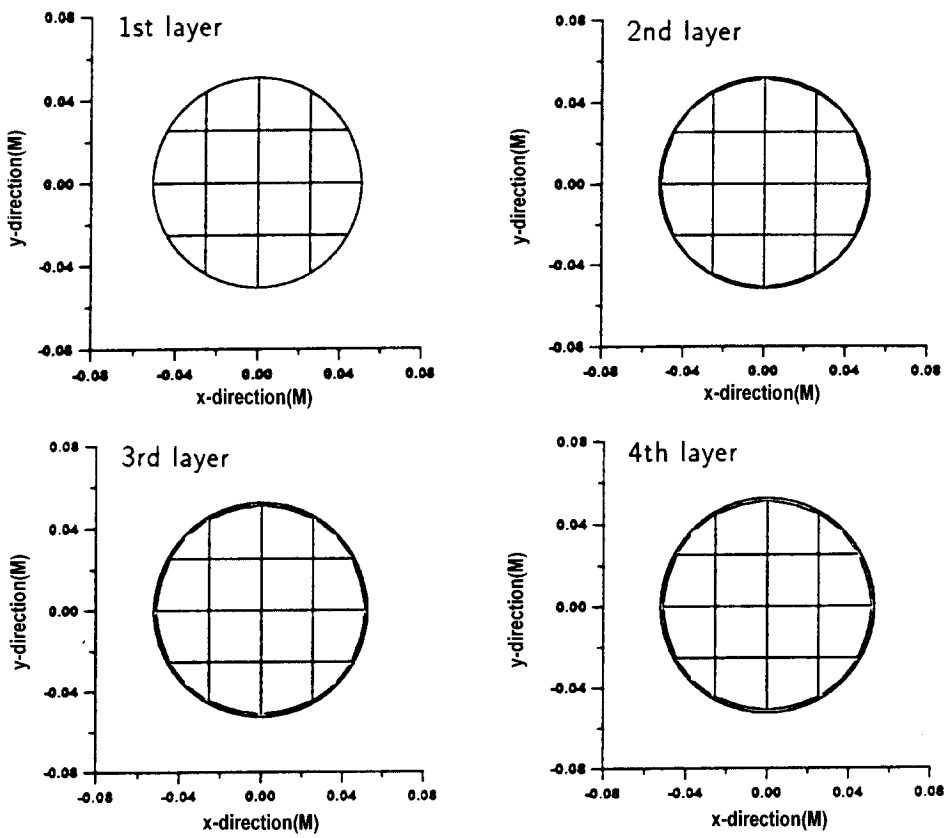

Fig. 3 Deformation due to the isotropic effect

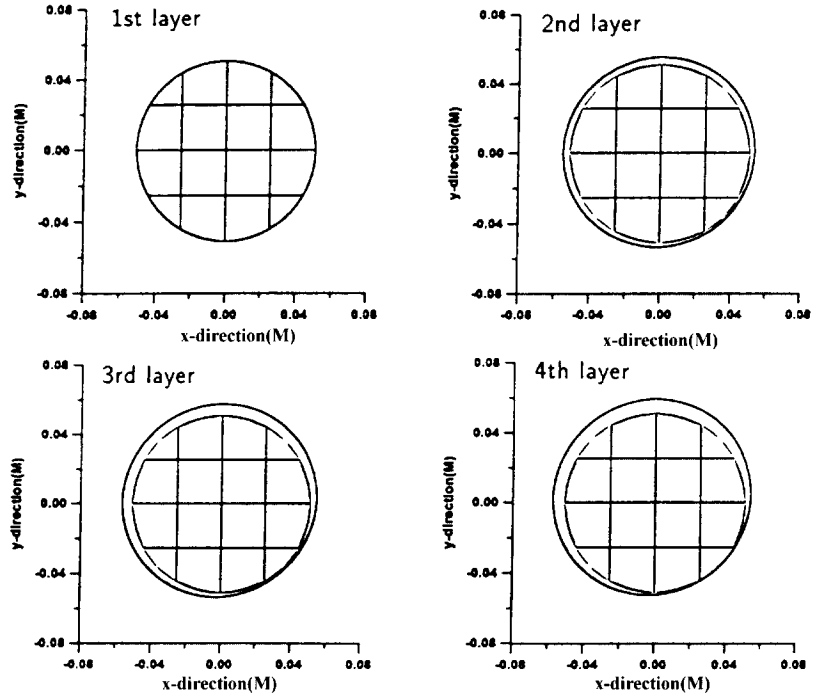

Fig. 4 Deformation due to the isotropic and deviatoric effects

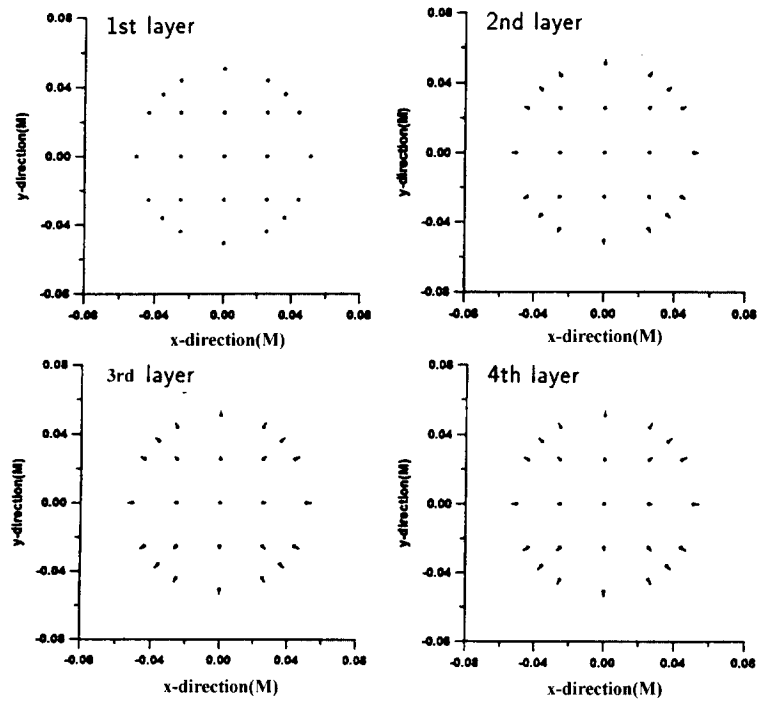

Fig. 5 Displacement due to the isotropic effect

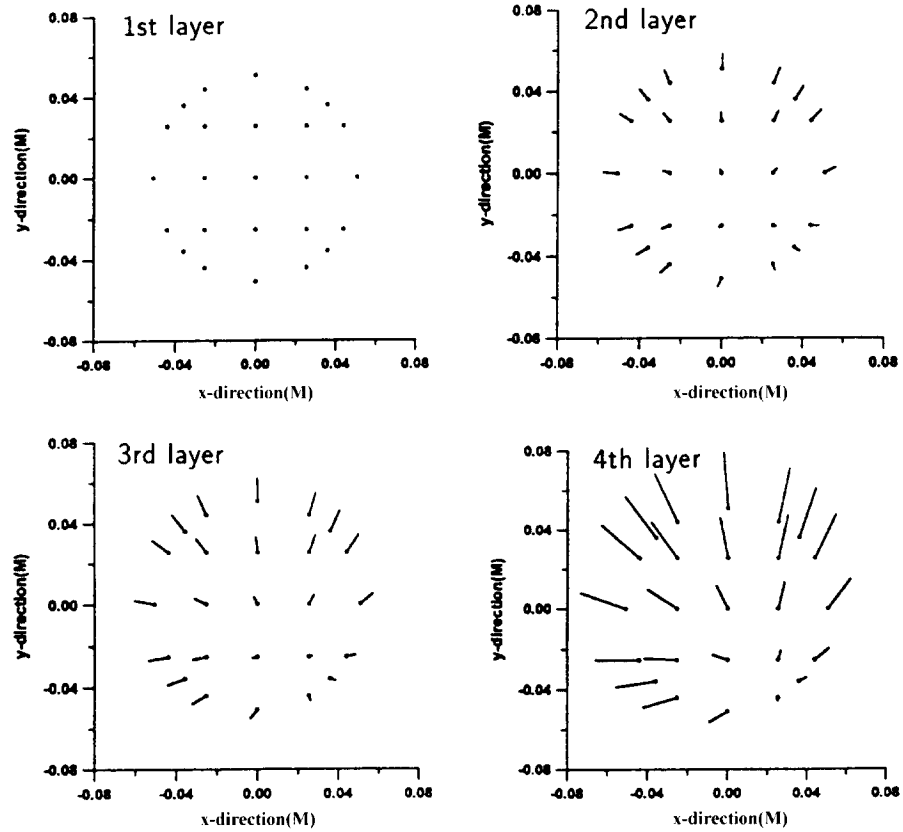

Fig. 6 Displacement due to the isotropic and deviatoric effects

obtained from the 200 steps. The diagram shows that more accurate results can be expected with more loading steps. The 200 loading steps are thus enough for obtaining a reasonable result.

Now for the specimen studied herein, the deformations in the *x-y* plane for the four layers are shown in Fig. 3 and Fig. 4. The tendency of a deformed cylinder under a specified loading can be viewed clearly from these plots. As the former plot presents the isotropic response without considering the deviatoric effect and a symmetric behavior is seen for the four layers. But when the deviatoric effect is added, as presentes in the latter plot, a nonsymmetric behavior is found for every layer. Similarly, if the displacements are blown up for the four layers, the effects of isotropic response and deviatoric response are seen clearly, as shown in Fig. 5 and Fig. 6, respectively. Note that the deformation and displacement were enlarged 600 times for better viewing, also the plots are shown for the *x-y* plane(no *z*-direction) only. It is found that the displacement of the 4th layer has higher value than the first layer due to compression and deviatoric effects. Also note that the present calculation divided the total external forces including plastic virtual force into several steps. Initially, elastic behavior is considered so the plastic pseudo-force is set to zero, and the Eq. (19) is used to obtain deformation in each node, where the resulting linear system equations are solved by Gauss-Jordan method. After required variables are calculated according to

definitions from the endochronic theory, the plastic pseudo-force of each element is then obtained from Eq. (18), and assembled forces can be used for the next step. Repeatedly for each step, the calculation will be terminated until the loading condition is completed. Due to the effect of added force or frictional force involved in each calculation step, the results may also explain why the reason of non-symmetric deformation and displacement patterns at different layers are shown in Fig. 4 and Fig. 6. Since the average results directly obtained from the endochronic theory itself may not show the variations of a deformed body in detail, the present finite element analysis with the presentation of three dimensional results may provide a better understanding for a deformed body under the specified loading conditions. The results may also be useful in the field of road engineering.

4. Conclusions

In the present study, a finite element model based on the incremental endochronic theory for flexible pavement materials has been developed. Three grid systems with eight-node isoparametric elements, and different loading steps were used to perform the calculations for a specimen of a circular cylinder. The uniaxial stress experimental results on an asphalt mixture at 60°C in SHRP conducted by University of California at Berkeley have been used to check the ability of the derived numerical model, and reasonable results have been obtained. Next, a further analysis for the three dimensional circular cylinder has been performed to reveal more mechanical behaviors of the materials. The present numerical results have shown the effects of isotropic response and deviatoric response in a three dimensional manner, which provides a better understanding for a deformed flexible material under the specified loading conditions, and which may be useful in a practical road design. Note that this study focussed on the development of the finite element models for flexible pavement materials. Further analyses on related fields, using the present numerical models, deserve further study.

References

Henrinksen, M. (1984),"Nonlinear viscoelastic stress analysis-a finite element apporach", *Computers and Structures,* **18**, 133-139.

Lee, C.F. (1995), "Recent finite element applications of the incremental endochronic plasticity", *Int. J. Plasticity,* **11**(7), 843-865.

Liu, M.L. (1993), "The structure response of pavement by using the hypoelastic model", The 17th Nat. Conf. Theo. Appl. Mech., Taiwan, 761-768.

Liu, M.L. (1994), "The use of hypoelastic constitutive model for asphalt concrete materials", Int. Compu. Meth. Strue. Geot. Engng., Hong Kong, 695-700.

Row, G.M., Brown, S.F., and Bouldin, M.J. (1995), "Visco-elastic analysis of hot mix asphalt pavement structures", Transportation Research Board 74th Annual Meeting, Washington D.C., Paper No. 95-0617.

SHRP Project (1991), "Performance-related testing and measuring of asphalt-aggregate interaction and mixtures", Quarterly Report, Part I - Technical Section, Institute of Transportation Studies, Asphalt Research Program, U.C. Berkeley, California, QR-UCB-A-003A-91-2.

Sugiura, K., Lee, G.C., and Wang, K.C. (1987), "Endochronic theory for structure steel under nonpropotional loading", *J. Engng. Mech.,* **113**(12), 1901-1917, ASCE.

Valanis, K.C. (1971), "A theory of viscoplasticity without a yield surface, part i. general theory, part ii. application to mechanical behavior of metals", *Arch. Mech.,* **23**, 511-517.

Valanis, K.C. (1980), "Fundamental consequence of a new intrinsic time measure: plasticity as a limit of the endochronic theory", *Arch. Mech.,* **32**, 171-191.

Valanis, K.C. and Fan, J. (1984), "A numerical algorithm for endochronic plasticity and comparison with experiment", *Computers and Structures,* **19**, 717-724.

Valanis, K.C. and Lee, C.F. (1984), "Endochronic theory of cyclic plasticity with application", *Trans. ASME, J Appl. Mech.,* **51**, 367.

Watanabe, O. and Atluri, S.N. (1986), "Internal time, general internal variable, andm multi-yield-surface theories of plasticity and creep: a unification of concepts", *Int. J. Plasticity,* **2**, 37-57.

Wu, H.C. and Aboutorabi, M.R. (1988), "Endochronic modeling of coupled volumetric-deviatoric behavior of porous and granular materials", *Int. J. Plasticity,* **4**, 163-18.

Wu, H.C. and Komarakulnanakorn, C. (1992), "On the limit case of endochronic theory", *Int. J. Solids and Structures,* **29**(2), 135-143.

Wu, H.C. and Lu, J.K. (1995), "Further development and application of an endochronic theory accounted for deformation induced anisotropy", *Acta Mechanica,* **109**, 11-26.

Wu, H.C. and Wang, P.T. (1983), "Endochronic description of sand response to static loading", *J. Engng. Mech.,* **109**, 970-989, ASCE.

Wu, H.C., Wang, P.T., Pan, W.F. and Xu, Z.Y. (1990), "Cyclic stress response of porous aluminum", *Int. J. Plasticity,* **6**, 207-230.